

Investigation of Corrosion Inhibition of Welan Gum and Neem Gum on Reinforcing Steel Embedded in Concrete

M.G.L. Annaamalai^{1,}, G. Maheswaran¹, N. Ramesh², C. Kamal³, G. Venkatesh³, P. Vennila⁴*

¹ Department of Civil Engineering, VSA Group of Institutions, Salem, Tamil Nadu, India.

² Department of Civil Engineering, KS Rangasamy College of Technology, Namakkal, Tamil Nadu, India.

³ Department of Chemistry, VSA Group of Institutions, Salem, Tamil Nadu, India.

⁴ Department of Chemistry, Thiruvalluvar Government Arts College, Rasipuram, Tamil Nadu, India.

*E-mail: annaamalaimgl@gmail.com

Received: 13 May 2018 / Accepted: 27 June 2018 / Published: 1 September 2018

Two naturally derived gums namely Welan gum (WG) and Neem gum (NG) have been tested for their anti-corrosion potential against the steel reinforced in concrete in NaCl media at different time interval using standard corrosion characteristic techniques such as electrochemical impedance spectroscopy (EIS), Tafel polarization study (PDS) and scanning electron microscopy (SEM). The results of EIS and PDS revealed the protective film forming potential and mixed type inhibitive action of both the two gums. In addition, the formation of protective layer over embedded steel surface has been suggested by SEM. The density functional theory (DFT) results indicated the active centers of inhibitor molecules which could be attached on embedded steel surface that influence the anti-corrosion ability of WG and NG. The durability properties viz., compressive strength and split tensile strength were also improved on the introduction of gums to the concrete. The mechanism of inhibition of corrosion of steel embedded in concrete in 3.5% NaCl solution by both the two gums has also been established.

Keywords: Welan gum, Neem gum, Electrochemical impedance spectroscopy, Tafel Polarization, Density Functional Theory, Reinforced steel.

1. INTRODUCTION

Iron and alloys of iron found enormous applications viz., construction, engineering, automobile and various industrial applications among all the other metals because of their significant functional properties and cost effective nature [1-7]. Concrete structures are generally made up of reinforcing steel bars in ingredients of concrete in order to retain the structure and the concrete materials properly.

However, these metals have a makeable demerit that they are readily undergo corrosion [6-12]. To overcome this problem, several researchers are being focused towards the development of greener and sustainable concrete structures, recent past. The use of synthetic organic compounds for inhibiting corrosion is one among the familiar techniques available for controlling the corrosion of metals in acid as well as neutral solutions. The problem of using organic inhibitors obtained from synthetic origin is that, they are very costly in addition to toxic nature [10-14]. Hence, there is a great necessity for the development of corrosion inhibitors from natural origin which are having a merit that they are bio-degradable as well as cost-effective too. Nowadays, several researchers developed number of natural based corrosion inhibitors to inhibit corrosion of metals in various media [7-14]. Also, there are enormous reports available in literature with a view to elaborating the development of durability characteristics of concrete by natural gums, which are added as viscosity modifying enhancers.

Viscosity-enhancing admixture (VEA) is being widely used in various applications in construction and building engineering. VEA (polysaccharides) are soluble in water that enhances the water holding ability of the paste, which is used in construction of building concrete particularly for the repairing the underground marine and hydraulic structure [13-17]. Some VEA can minimize the risk of isolation of the heterogeneous ingredients present in concrete while transport, dislocate and accumulate of it and which provided improved stability to the cast concrete in a plastic state. In addition, it could be gained while the consistencies of the concrete subjected to flow is enhanced or at the time of concrete directed to very high shear rate, occurred in pumping as well as consolidation.

Several researchers proved that, natural gums viz., WG, guar gum, NG, gum Arabic Karroo etc., are used as a VEA in various types of concrete structures. Khayat et al., have reported the effect of WG-superplasticizer blends on cement grouts properties [10]. Xu and his co-workers reported the comparative and valuable information of rheological properties of WG and xanthan gum in aqueous media [11]. Mbugua et al. reported the influence of gum arabic karroo on water-reducing process concrete mortar [12]. Natural gums are being used as inhibitors against corrosion of various metals in various solutions. Research group of Messali have reported that, guar gum has been efficiently inhibit corrosion of carbon steel in H_3PO_4 solution [13]. Azzaoui and his co-workers developed the green corrosion inhibitor (gum arabic) from the natural origin for the corrosion of mild steel in acid solutions [14]. Biswas and his co-workers reported the inhibitive ability of gum acacia against acidic corrosion of mild steel [15]. Further, they were also examined the xanthan gum in addition to its graft co-polymer for their anti-corrosion effect. Addition to this, xanthan gums inhibitive effect along with synergism effect for the corrosion of mild steel has also been evidenced by research group of Mobin [16]. Bentrach and his co-workers have studied gum arabic against steel pipeline corrosion in HCl medium [17]. Research group of Alwaan have studied the anti-corrosive nature of polymer derived from a tree namely Iraqi apricot on mild steel corrosion in acid solution [18]. Research group of Peter have reported the anti-corrosion action of various natural gums on metals in various types of solutions [19]. But, there are very primitive studies have been included in the literature in view of enhancing mechanical properties as well as anti-corrosion ability, simultaneously.

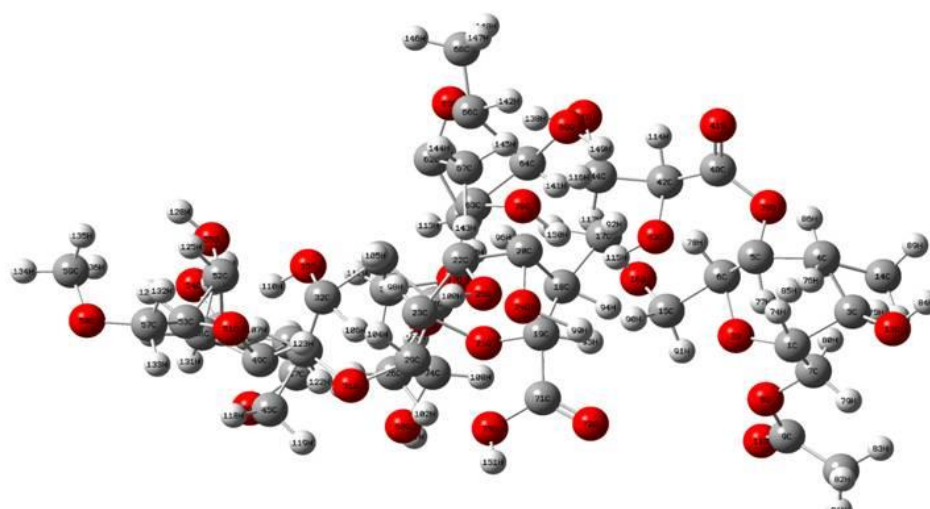
A detailed perusal of literature review on gum admixtures revealed the inhibitive ability of gums on corrosion of various metals in various kinds of solutions in addition to the development of mechanical properties of concrete. So, the development of gums from natural sources as admixture for concrete will

enhance the lifetime and the durability characteristics of concrete structures. Hence, in order to develop gums as affordable natural admixtures with a view to enhance viscosity and improve anti-corrosive concrete structures, the well known natural gums viz., WG and NG have been tested for their potential in the present study.

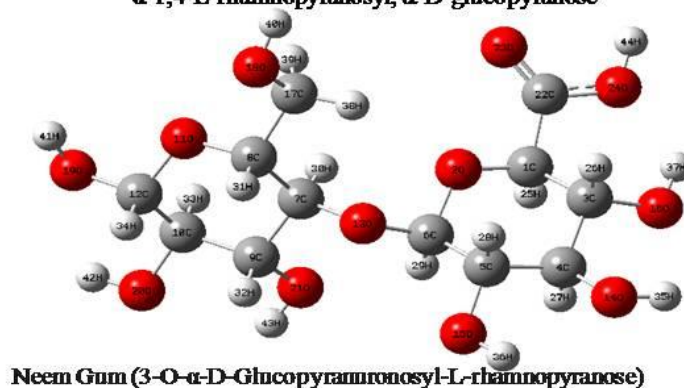
The study includes electrochemical measurements (EIS and PDS) of steel reinforced in concrete in absence and presence of various concentrations of natural gums. Further, the mechanical properties (compressive and split tensile strengths) of concrete without and with different concentrations of natural gums have also been carried out. In addition, theoretical calculations are considered to determine the molecular structure with a view to establish the electronic structure and monomer reactivity sites of inhibitors. Using molecular mechanics, the exact kind of adsorption of monolayer produced by the inhibitor molecule over the surface metal can well be understood by the analysis of interfacial configuration, interaction of monolayer with metal surface and cohesive energy of monolayer.

2. EXPERIMENTAL

2.1 Collection of gums



Pentasaccharide (Welan gum): β -1,3-D-glucopyranosyl, β -1,4-D-glucuronopyranosyl, β -1,4-D-glucopyranosyl, α -1,4-L-rhamnopyranosyl, α -D-glucopyranose



Neem Gum (3-O- α -D-Glucopyranranosyl-L-rhamnopyranose)

Figure 1. The optimized structure of natural gum monomer using 6-311G++(d,p)

The gum of Welan tree and Neem tree were collected from the forest region of Salem district, Tamil Nadu. The collected gum samples have been identified by the expert taxonomist in the Botanical Survey of India, Agriculture University campus, Coimbatore, Tamil Nadu, India. The specimens as vouchers (BSI /SRC/5/23/2016/TECH/166) are made available in the Department of Civil Engineering, VSA group of Institutions, Salem for further reference. The monolayer structures of WG and NG are shown in Fig.1.

2.2 Preparation of concrete block samples

The concrete block samples were prepared by following the same process as reported earlier. Samples were prepared using Portland cement, aggregate and water and reinforcing steel according to standard (IS 10262-1982) have been used throughout the study [12-15]. The dimension of prepared concrete blocks is as follows, 150 x 100 x 100 mm. Each and every block was made using cement, sand and gravel with the ratio of 1:2:4 (C:S:G). All the rebar were abraded appropriately prior to each preparation, in order to remove unwanted mill scale and rust stains occurred on the surface of steel rebar. Then, they were inserted symmetrically across the length of the block and they covered by 42mm concrete. 140 mm the of brass upon 160 mm were buried in concrete and the rest 20 mm left out for electrical connection. The concrete blocks prepared without addition of powdered gums were used as control (blank) specimens. For the preparation of testing concrete samples, desired amount of powdered gums were dissolved in water to prepare concrete samples including various concentrations of WG and NG. All the specimens were tested in 3.5% NaCl solutions.

2.3 Electrochemical investigation

The anticorrosion properties of WG and NG were evaluated using the electrochemical methods namely PDS and EIS [6-10]. All the experiments have carried out using three cell setup (C=0.37, S=0.017, Mn=1.21, P=0.021, Si=0.23, Cu=0.016, Ni=0.02, Cr=0.02, V=0.003 and remaining Fe %) which includes standard calomel electrode as reference electrode, platinum wire as auxiliary electrode and steel reinforcing in concrete as working electrode. The steel was reinforced in cement concrete without and with various concentrations of natural gums (WG and NG) and they were immersed in NaCl solution accordingly for various immersion time. The cell setup was left to be remained unchanged for a while to attain steady state prior to each measurement. All the measurements have been performed in CHI (760D plus) electrochemical work station operated along with CHI 760D plus software. The operating frequency range for EIS measurements was 0.01 Hz to 100000 Hz with 2 mV sine wave a.c. voltage excitation. EC-Lab SP300 software has been utilized to draw and analyze the impedance data. The calculation of double layer capacitance (C_{dl}) and charge transfer resistance (R_{ct}) from Nyquist plots were done as described earlier [20-24]. The potential of the setup has been evaluated using the PDS curves, which were recorded at 0.5 mVs^{-1} sweep rate. The potentials were varied along with the corrosion potential in the direction of the cathodic to the anodic side. The corrosion potential and corrosion current densities have been calculated from the curves.

2.4 SEM images

Reinforced steel specimens prepared with a dimension of 1 x 1 x 0.1 cms were buried in concrete in absence and presence of admixtures for about 28 days. Then, the steel specimens inserted in concrete were carefully removed and washed well using doubly distilled water prior to drying. SEM images were recorded in VEGAS-TESCAN scanning electron microscope [21].

2.5 Compressive and split tensile strength

The mechanical strengths including compressive and split tensile strengths were determined by following the standard procedure (IS 10262-2009) for concrete samples with and without different concentrations WG and NG universal testing machine.

2.5 Theoretical calculations

The main monomer of natural gum (WG and NG) were completely optimized by Gaussian 09w software using B3LYP/6-311(d,p), functional and structure were projected by Gauss view 05 software [25, 26]. After that, the geometry optimized monomers are utilized to calculate physico-chemical parameters in various phases (Gas & Water) and various levels viz., B3LYP/321, B3LYP/6-31G and B3LYP/6-311G++ (d,p).

The physico-chemical parameters namely HOMO, LUMO, ΔE, ionization Potential Energy (IE), electron affinity (EA) electronegativity (χ) global hardness (η) and electrons transferred (ΔN) have been computed [27-32] and discussed by means of anti-corrosion potential.

$$\chi = -\mu = \frac{I + A}{2} \text{----- (1)}$$

$$\eta = \frac{I - A}{2} \text{----- (2)}$$

$$\mu = \frac{EA + IE}{2} \text{----- (3)}$$

$$\eta = \frac{EA - IE}{2} \text{----- (4)}$$

The absolute softness (σ) is a magnitude of electrons polarized in the cloud of chemical species and also which referred the inverse of global hardness.

$$\sigma = \frac{1}{\eta} \text{----- (5)}$$

Electrophilicity index (ω) are derived the following relationship and nucleophilicity (ε) is the inverse of the electrophilicity (ω = 1/ε).

$$\omega = \frac{\mu^2}{2\eta} = \frac{\chi^2}{2\eta} \text{----- (6)}$$

The fraction of transference electrons (ΔN) towards the metal from inhibitor has been calculated using the equation:

$$\Delta N = \frac{\chi_{Fe} - \chi_{inh}}{2(\eta_{Fe} + \eta_{inh})} \text{-----}(7)$$

where, χ_{Fe} and χ_{inh} are the electronegativity of metal and inhibitor, respectively meanwhile η_{Fe} and η_{inh} are the hardness of metal and inhibitor, respectively. A value of 7 eV/mol was used for the χ_{Fe} , while η_{Fe} was equated to 0 eV/mol for bulk Fe atom.

3. RESULTS AND DISCUSSION

3.1 Electrochemical Measurements (PDS & EIS)

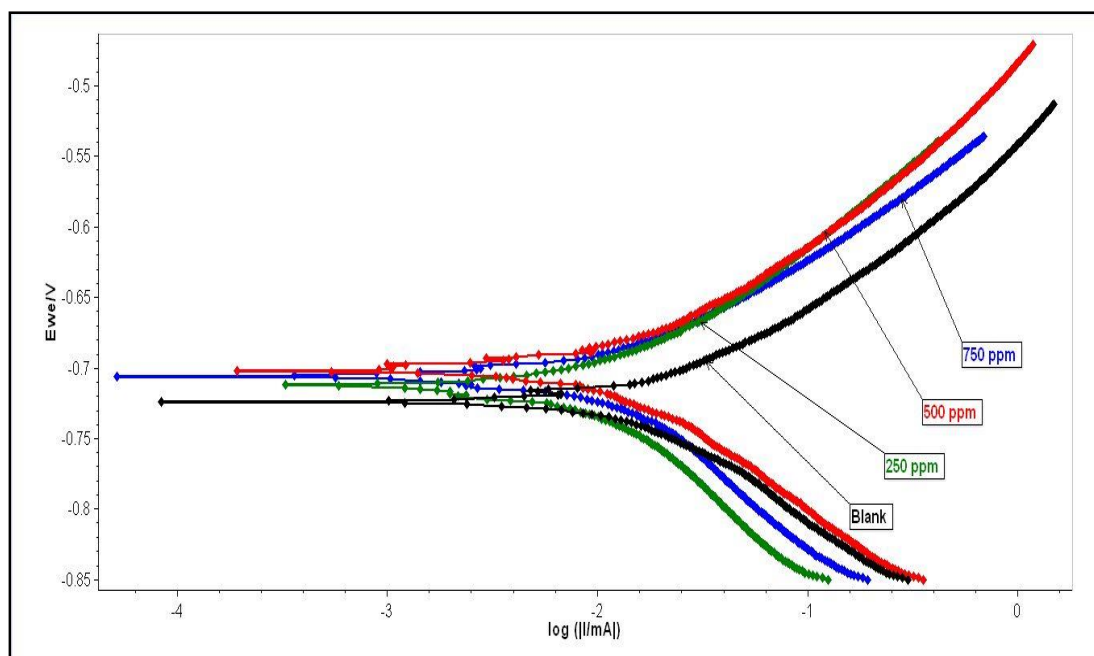


Figure 2. Tafel plots of embedded steel in concrete without and with NG 120 days

The PDS curves were obtained in the sweep rate of about 0.5 mVs^{-1} . The potentials were varied from cathodic direction towards the corrosion potential and simultaneously towards anodic range. The PDS curves of reinforced steel in absence and presence of various concentrations of WG and NG in chloride media are shown in Fig.2 and 3 and electrochemical parameters viz., corrosion potential (E_{corr}), corrosion current density (I_{corr}), inhibition efficiency (%IE) and Tafel constants (b_a and b_c) of from Tafel curves are listed in Table 1 & 2. Inhibition efficiency was calculated using the following equation,

$$IE(\%) = \frac{(I_{corr} - I_{corr(i)}) \times 100}{I_{corr}} \text{-----}(8)$$

where, I_{corr} is the corrosion current density of uninhibited specimen whereas $I_{corr(i)}$ is the corrosion current density of inhibited specimens. They were obtained by extrapolating Tafel lines to the corrosion potential.

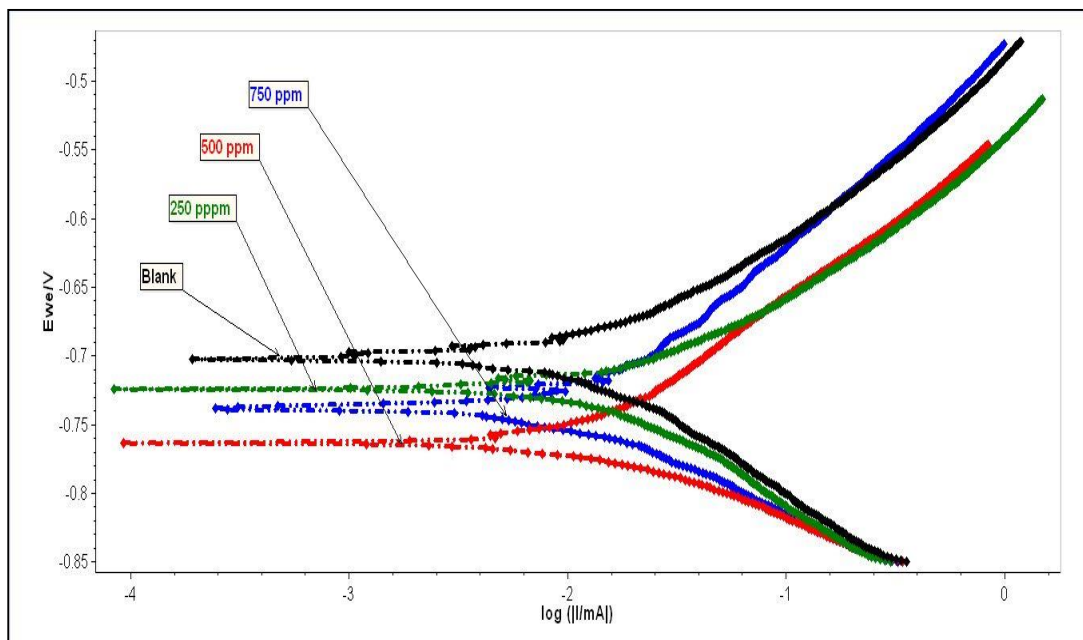


Figure 3. Tafel plots of embedded steel in concrete without and with WG 120 days

Table 1. Effect of Welan gum on reinforced steel in Neutral media (PDS)

S. No.	Concentration of gum (ppm)	b_a $mVdec^{-1}$	b_c $mVdec^{-1}$	E_{corr} mV	I_{corr} μAcm^{-2}	% of IE
1	0	124	122	-723	1318	-
2	250	136	105	-738	701	47
3	500	125	111	-763	386	71
4	750	121	116	-725	197	85

Table 2. Effect of Neem gum on reinforced steel in Neutral media (PDS)

S. No.	Concentration of gum (ppm)	b_a $mVdec^{-1}$	b_c $mVdec^{-1}$	E_{corr} mV	I_{corr} μAcm^{-2}	% of IE
1	0	124	122	-723	1318	-
2	250	119	122	-719	753	42
3	500	111	125	-709	415	68
4	750	107	113	-714	226	82

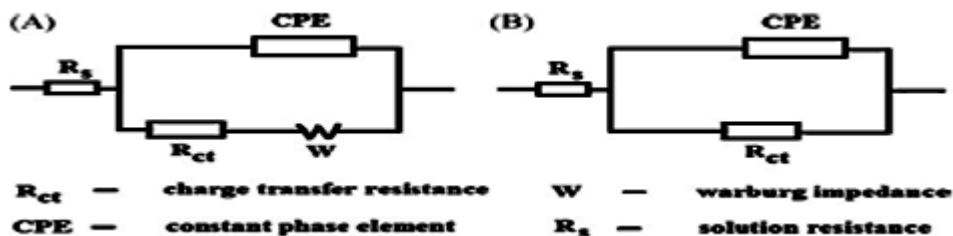


Figure 4. Equivalent circuits

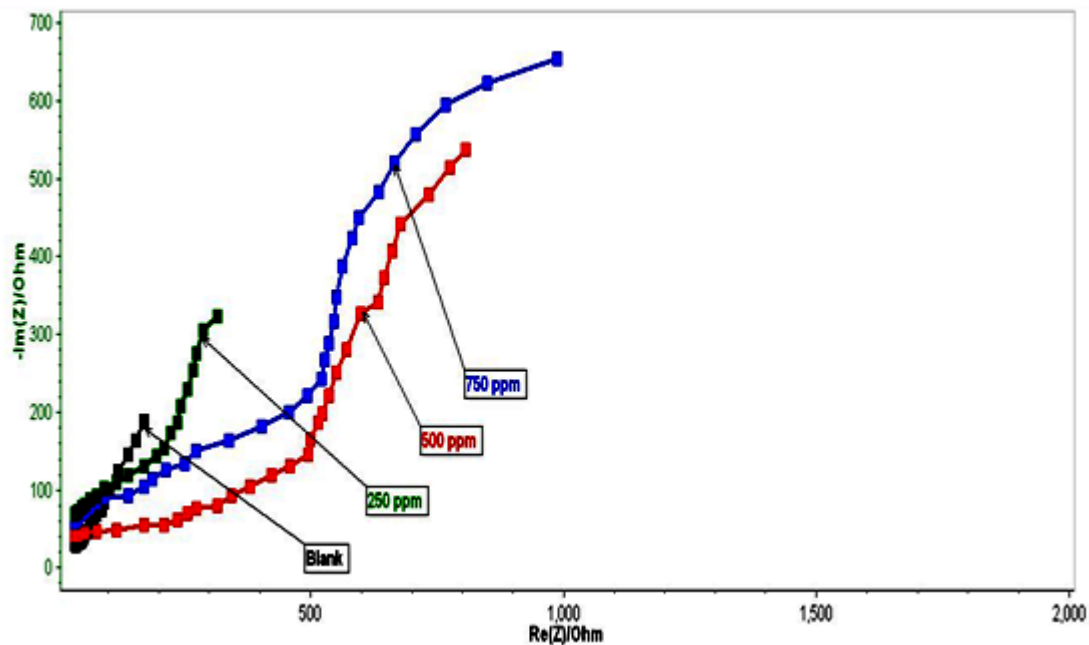


Figure 5. Nyquist plots of embedded steel in concrete NG 120 days

The results obviously showed that, both the gums were suppressed the corrosion current densities without altering the values of corrosion potential and is an indicative of mixed type inhibition. It is further observed that, *ba* and *bc* values did not fall on any particular direction and is supported the mixed mode action of the studied gums. The equivalent circuit (Fig.4) diagram corresponding to EIS is presented as Fig.5 and 6 [34, 35]. Where R_{Ω} represents resistance of solution, R_t is resistance of corrosion product and C_{dl} is the capacitance of double layer.

The Nyquist plots for the impedance behavior of reinforced steel in chloride media without and with introduction of several corresponding concentrations of both WG and NG are given in Fig.5 and 6. It is clear from the figures that, addition of gums enhanced the R_{ct} accordingly and suppressed C_{dl} . These variations in values could be responsible for the rise in electrical double layer's thickness [36].

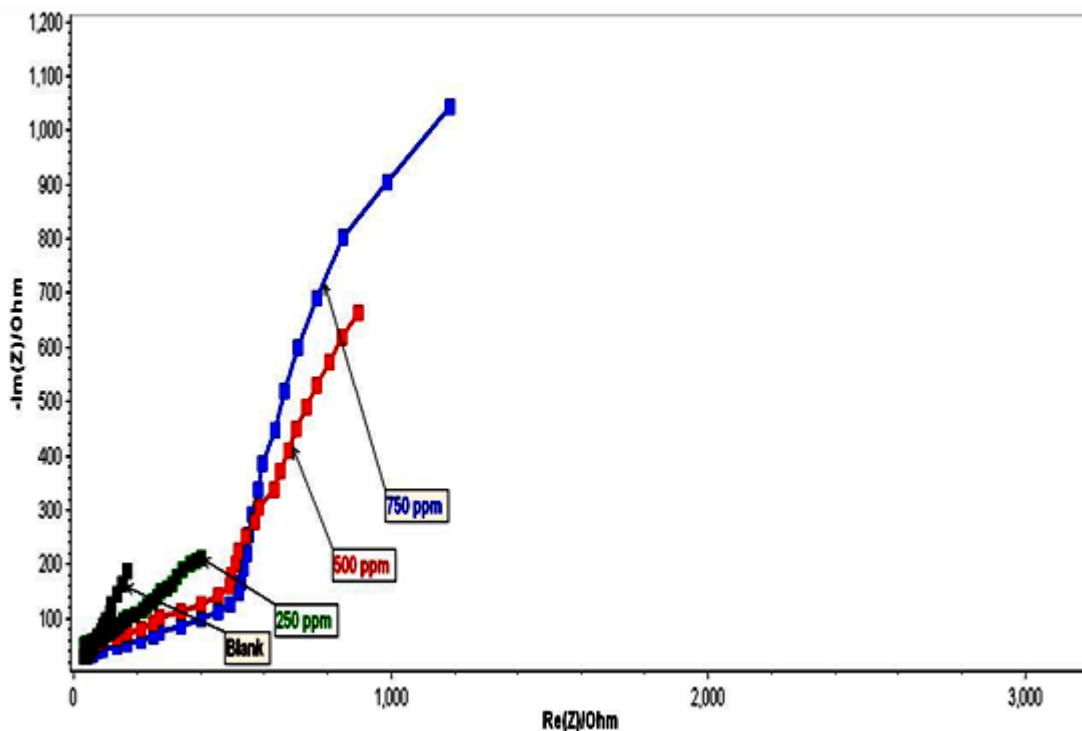


Figure 6. Nyquist plots of embedded steel in concrete WG 120 days

Table 3. Effect of WG on reinforced steel in neutral media (EIS)

S. No.	Concentration of gum (ppm)	R_{ct} $\Omega \text{ cm}^{-2}$	C_{dl} μFcm^{-2}	n	% of IE
1	0	143	246	0.8893	-
2	250	368	187	0.8342	61
3	500	857	145	0.6964	83
4	750	1164	122	0.6457	87

Table 4. Effect of NG on reinforced steel in Neutral media (EIS)

S. No.	Concentration of gum (ppm)	R_{ct} $\Omega \text{ cm}^{-2}$	C_{dl} μFcm^{-2}	n	% of IE
1	0	143	246	0.8893	-
2	250	285	192	0.8257	49
3	500	763	153	0.6812	81
4	750	946	137	0.6235	84

The observation of increased R_{ct} values is an indication of the production of surface protective film between the metal and solution (interface double layer). The results suggested that both the two examined gums (WG and NG) were adsorbed over the surface of metal thereby decreasing C_{dl} values and rising R_{ct} values [37]. R_{ct} , C_{dl} and inhibition efficiency were calculated from EIS curves using following equations and they are given in Table 3 & 4.

$$IE = \frac{R_{ct(i)} - R_{ct(b)}}{R_{ct(i)}} \text{----- (9)}$$

where $R_{ct(i)}$ and $R_{ct(b)}$ are charge-transfer resistance values in presence and absence of the inhibitor, respectively. The different inhibitor performances have been compared and listed in Table 5.

Table 5. Inhibition efficiency of various natural inhibitors

Plant Extract	Specimen	IE (%)	Reference
<i>Justicia gendarussa</i>	Steel carbon	78	38
<i>Anthocleista djalonensis</i>	Steel carbon	85	39
<i>Prosopis juliflora</i>	Steel carbon	91	20
<i>Ricinus communis</i>	Steel carbon	87	40
Welan gum	Steel carbon	87	This work
Neem gum	Steel carbon	84	

3.2 Quantum chemical calculations

DFT based on the quantum chemical calculations were proved as efficient technique in determining the inhibition ability of molecules based on their reactivity and their tendency to inhibit metal corrosion. The FMOs highly contribute in the detection of active centers responsible for the adsorption of molecules. The corrosion inhibitors donate electrons to the vacant orbitals of surface of metal as well as gain free electron from metal surface. The ability of inhibitors can well be understood with frontier molecular orbital of HOMO and LUMO. The HOMO is associated with donating potential of electron and LUMO is responsible for the accepting potential of electron [8, 20, 41 and 42]. Fig.7 is clearly indicated the donating and accepting ability of electrons of inhibitor and metal. HOMO and LUMO values revealed the interaction of inhibitor molecule with metal surface. HOMO-LUMO energy is associated with reactivity. From Tables 6 & 7, it can be seen that, both the gums have lower value of ΔE which indicated that, they are easily polarizable and readily absorbed on the metal surface. The energy of HOMO and LUMO are in accordance with ionization potential and electron affinity, respectively. They characterize the vulnerability of molecules towards attack with electrophile and nucleophile. The properties of molecules such as stability and reactivity are determined by hardness and softness values. Generally, molecules having lower hardness are tending to have higher inhibitive ability. The volume of molecule is directly related to the dipole moment (μ), which increases the available surface area to make interaction among molecule and metal surface and increased the corrosion inhibition.

Table 6. Physico-chemical parameters calculated using DFT method for Pentasaccharide (Welan gum): β -1,3-D-glucopyranosyl, β -1,4-D-glucuronopyranosyl, β -1,4-D-glucopyranosyl, α -1,4-L-rhamnopyranosyl, α -D-glucopyranose [43].

DFT/Functional	Gaseous Phases									
	E_{HOMO}	IE	E_{LUMO}	EA	ΔE	χ	η (eV)	σ (eV)	ω	ϵ
B3LYP/321	-7.76	7.76	-1.16	1.16	-6.61	4.46	3.31	0.31	3.06	0.33
B3LYP/6-31G	-8.09	8.09	-1.22	1.22	-6.88	4.66	3.44	0.29	3.15	0.32
B3LYP/6-311G++(d,p)	-9.32	9.32	-2.65	2.65	-6.68	5.99	3.34	0.31	5.36	0.19
Aqueous Phases										
B3LYP/321	-11.12	11.14	-1.07	1.07	-10.08	6.11	5.04	0.20	3.71	0.27
B3LYP/6-31G	-11.47	11.47	-1.28	1.29	-10.18	6.38	5.09	0.19	3.82	0.25
B3LYP/6-311G++(d,p)	-12.58	12.58	-2.72	2.72	-9.87	7.65	4.94	0.20	5.93	0.17

Table 7. Physico-chemical parameters calculated using DFT method for 3-O- α -D-Glucopyranuranyl-L-rhamnopyranose (NG)

DFT/Functional	Gaseous Phases									
	E_{HOMO}	IE	E_{LUMO}	EA	ΔE	χ	η (eV)	σ (eV)	ω	ϵ
B3LYP/321	-7.28	7.28	-2.14	2.13	-5.15	4.71	2.57	0.39	4.31	0.24
B3LYP/6-31G	-10.75	10.75	-2.99	2.99	-7.77	6.87	3.88	0.26	6.08	0.17
B3LYP/6-311G++(d,p)	-7.03	7.03	-0.96	0.96	-6.07	4.01	3.04	0.33	2.63	0.38
Aqueous Phases										
B3LYP/321	-10.72	10.72	-2.21	2.21	-8.52	6.46	4.26	0.24	4.90	0.20
B3LYP/6-31G	-14.13	14.13	-3.06	3.06	-11.07	8.60	5.54	0.19	6.667	0.16
B3LYP/6-311G++(d,p)	-10.24	10.24	-0.99	0.99	-9.25	5.62	4.63	0.22	3.41	0.29

Electrophilicity index (ω) is contributed to the electron accepting nature of inhibitor molecules. It is a magnitude of the stabilization energy after accepting excess electron charge (ΔN) from the environment. The theoretical results of monomer (WG and NG) showed them as good inhibitors, meanwhile the comparison of calculated data suggested that, WG (monomer) showed better performance than NG (monomer) according to IE and ΔN values.

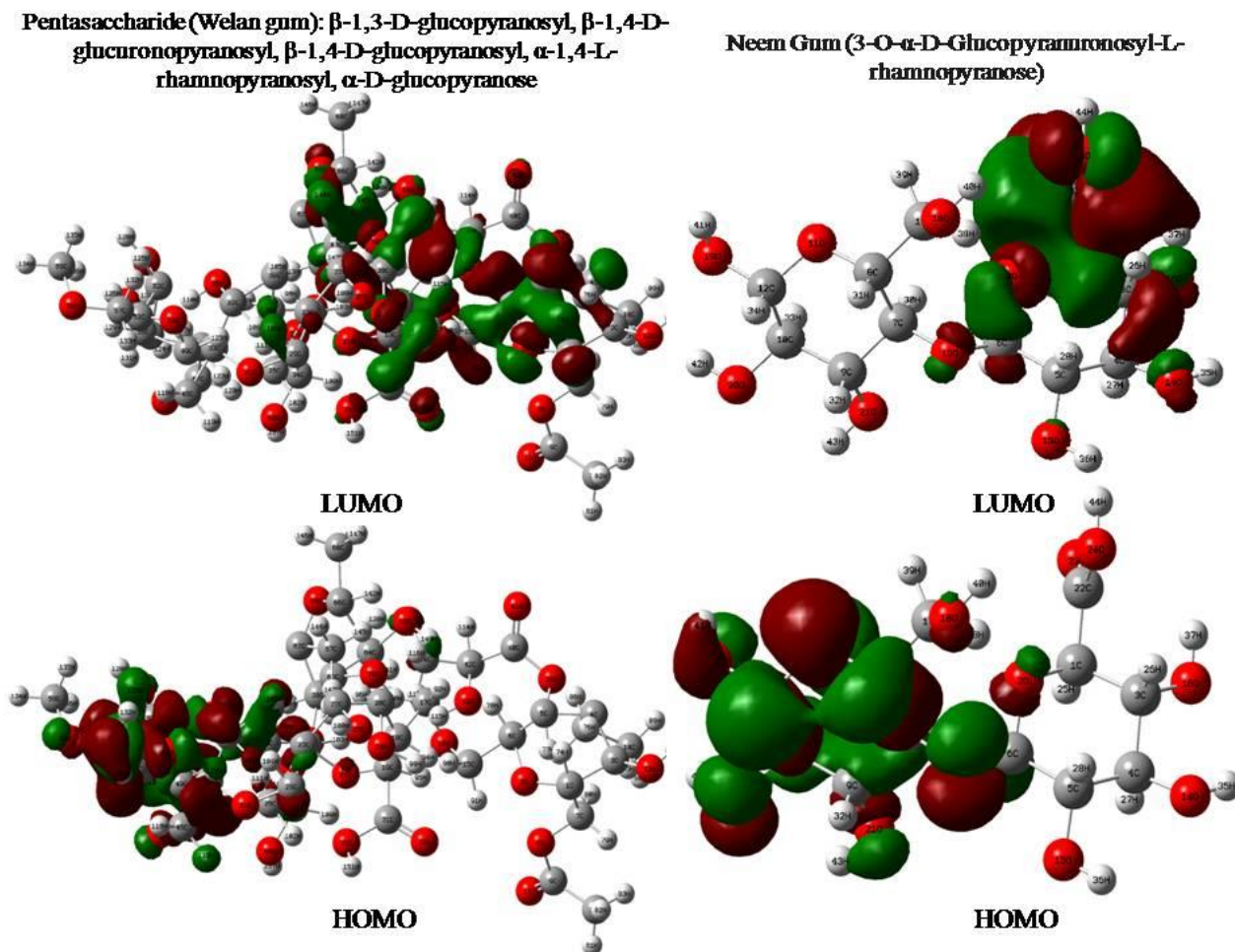


Figure 7. Representation of the orbital involved in the electronic transition of Natural gum monomer using 6-311G++(d,p)

3.3 Compressive Strength

Compressive strength of concrete samples after the addition of WG and NG has been calculated by following standard procedure using universal testing machine. The results showed that, addition of two gums increased the strength of admixture concrete than that of plain concrete. From the Table 8, it can be seen that, WG exhibited better strength than NG. The compressive strength of concrete cubes is evaluated at the age of 7, 14, 28 and 120 days and is provided in Table 8.

Table 8. Compressive strength of cube Specimens (N/mm²) 7, 14, 28 and 120 days

Days	7 Days		14 Days		28 days		120 days	
%	Welan Gum	Neem Gum	Welan Gum	Neem Gum	Welan Gum	Neem Gum	Welan Gum	Neem Gum
0	30.4		34.3		36.2		38.3	
250	32.6	32.2	35.4	34.9	38.5	37.7	39.5	38.6
500	33.3	32.7	38.7	38.2	40.8	40.2	41.5	40.4
750	35.6	35.6	38.5	38.4	40.6	40.4	42.7	42.2

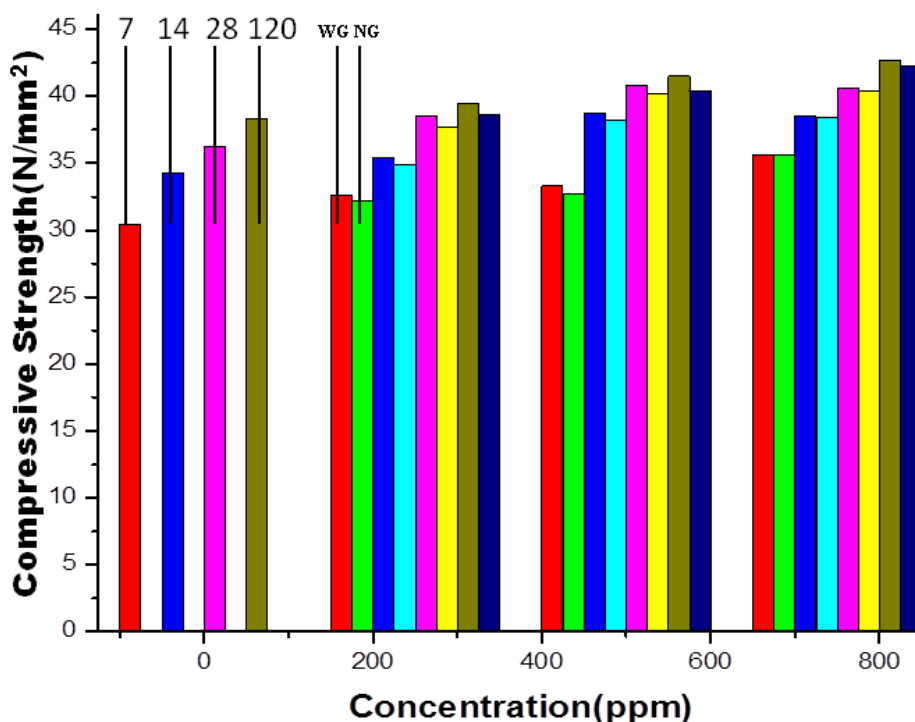


Figure 8. Variation of compressive strengths of concrete with and without WG and NG

From the Fig.8, it is clear that, the compressive strengths of the concrete have been increased gradually with the increase in natural gums concentration. There has been an increase in compressive strength obtained for concrete admixed with various concentrations (250, 500, 750 ppm) of two gums than conventional concrete. However, higher strength has been obtained for WG than that of NG.

3.4 Split Tensile strength

For split tensile test, the specimens were prepared as same as compressive test specimens. Fig.9 and Table 9 showed various tensile strengths of cylindrical specimens moulded using natural gums [9-12]. From the Fig.9, it is observed that, with the increased concentration of natural gums at the age of 7, 14, 28 and 120 days, the tensile strength of different concentration 250, 500 and 750 (ppm) were increased. Further, it is observed that, WG admixture concrete showed slightly higher strength than NG admixture concrete.

Table 9. Split Tensile Strength variations (N/mm²) 7, 14, 28 and 120 days

Days	7 Days		14 Days		28 days		120 days	
%	Welan Gum	Neem Gum						
0	1.82		2.14		2.72		3.12	
250	1.86	1.84	2.16	1.96	2.74	2.62	3.17	2.87
500	1.92	1.91	2.42	2.24	2.82	2.71	3.24	2.96
750	1.98	1.96	2.64	2.44	2.88	2.82	3.35	3.01

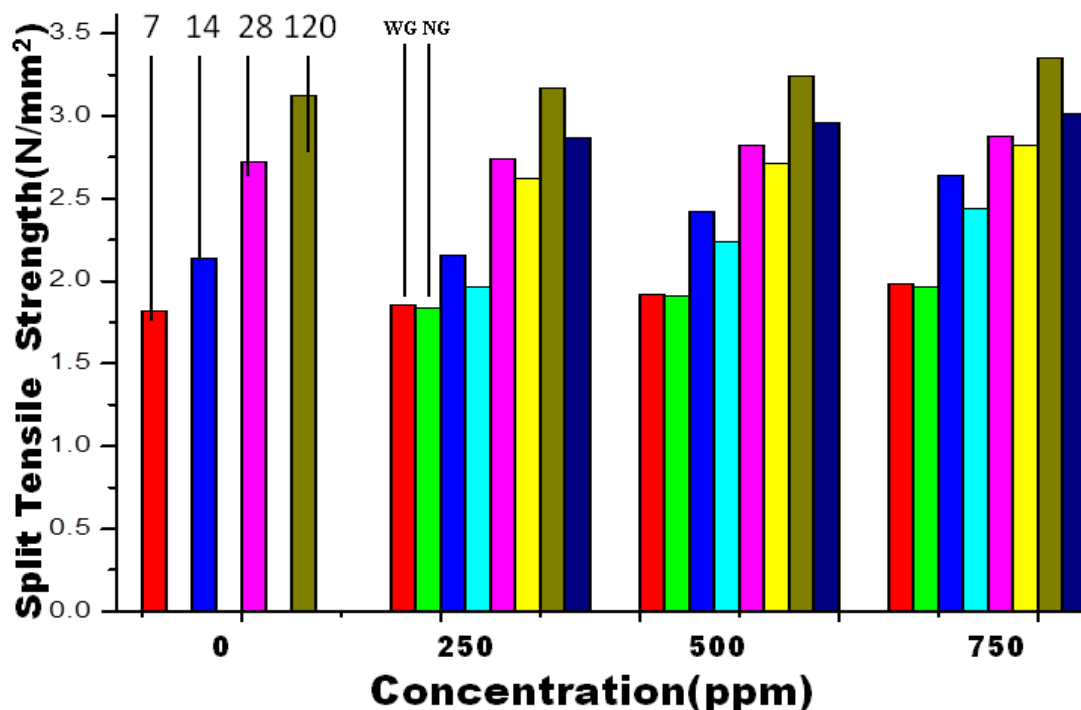


Figure 9. Variation of split tensile strengths of concrete with and without WG and NG

3.5 Scanning electron microscope (SEM)

To validate the results observed from earlier characterizations and to analyze the surface protection provided by the inhibitor molecules at a microscale range, the SEM images have been recorded for embedded steel in concrete in absence and presence of WG and NG with a particular immersion period and they are shown Fig.10-12.

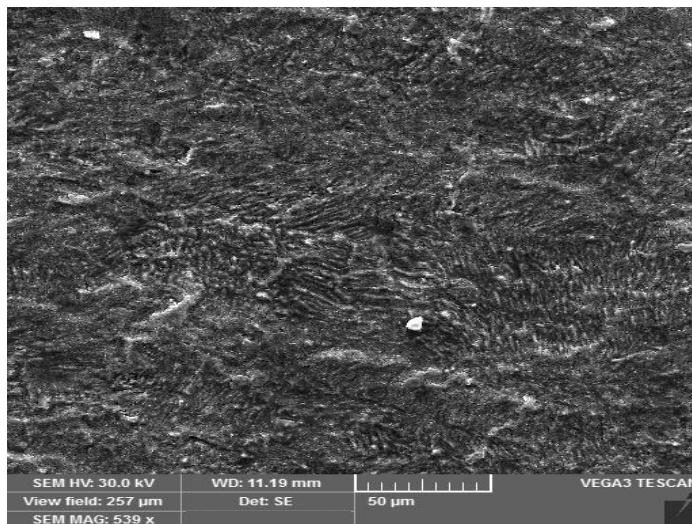


Figure 10. SEM image of control concrete (Blank)

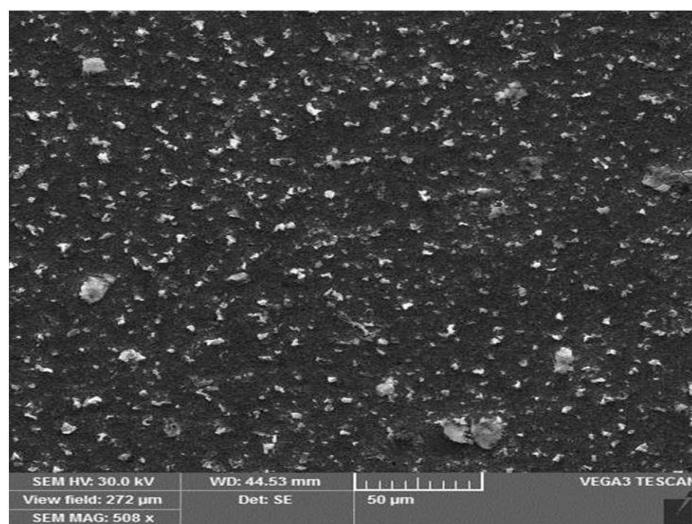


Figure 11. SEM image of concrete with WG

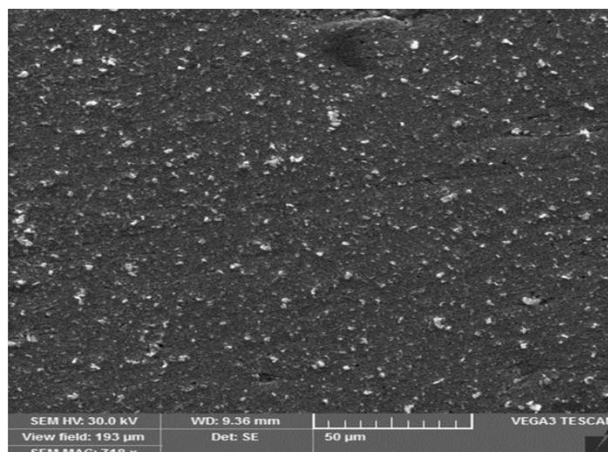


Figure 12. SEM image of concrete with NG

It can be seen clearly from the figures that, the surface of reinforced steel in absence of inhibitor has been damaged severely by the aggressive chloride ions. The surfaces of reinforced steel in presence of WG and NG are highly protected and less damaged, which could be due to the formation of protective film. This observation supported the results of EIS measurements [24].

3.6 Mechanism of Inhibition

Adsorption of inhibitor molecules occurred on the metal surface could be either physically or chemically adsorption. For the adsorption occurred physically, there must be a weak interaction between metal surface and inhibitor molecules (e.g. dipole-dipole interactions). In other words, chemical adsorption (chemisorption) happened by the sharing electrons of inhibitor molecules with metals, or the transmittance of charges/electrons from the inhibitor to the surface of metal [42, 44-46]. Considering the chemical structures of most naturally occurring inhibitors, there are many types of adsorptions.

Physisorption-The metal surface changed as negatively charged since anions of solutions adsorbed over the surface. Hence, the electrostatic interaction between negatively charged surface and positively charged inhibitor molecule has been occurred and retarded the anodic dissolution of iron.

Chemisorption-According to the donor-acceptor interaction concept, pi-electrons of the benzene rings which are mostly present in the natural inhibitor molecules can make interaction to the vacant d-orbital of the metal [46-51].

Chemisorption-The hydroxyl of the inhibitors can be adsorbed over metal surface via H-bonding, involving the dislocation of water molecules from the surface of metal. The adsorbed natural gums on the surface of metal form a protective film, which protects the metal surface from the aggressive ions attack.

4. CONCLUSIONS

The introduction of WG and NG to the concrete markedly inhibited the corrosion of reinforced steel in NaCl solution. The corrosion inhibition of steel embedded in concrete in NaCl solution via the

formation of protective film has been confirmed from the results of EIS and is further supported by SEM analysis. The results of PDS indicated the gums as mixed type inhibitors which could be attributed to the alteration of both the cathodic as well as anodic reactions. The mechanical properties viz., compressive strength, and split tensile strength have been increased with the addition of WG and NG to the concrete mortar. The results of DFT indicated that, the presence of active electron donating centre could be the main reason for the corrosion inhibition ability of WG and NG.

References

1. M. Vishnudevan and K. Thangavel, *Anti-corros. Methods Mater.*, 53 (2006) 271-276.
2. J.E. Slater, *Corrosion of Metals in Association with Concrete*, ASTM STP 818, Philadelphia, PA, 1983.
3. L. Li, A and A. Sagues, *Corros.* 60 (2004) 195.
4. M. F. Hurley and J. R. Scully, *Corros.*, 62 (2006) 892.
5. A. Ali Gürten, K. Kayakırılmaz and M. Erbil, *Constr. Build. Mater.*, 21 (2007) 669-676.
6. S.B. AL-Amoudi, M. Maslehuddin, A.N. Lashari and A.A. Almussallam, *Cem.Concr.Compos.*, (2003) 439-449.
7. A.S. Fouda, G. Elewady, K. Shalabi and H.A. El-Aziz, *RSC Adv.*, 5 (2015) 36957-36968.
8. A. S. Fouda, Y. A. Elewady, H. K. Abd El-Aziz and A. M. Ahmed, *Int. J. Electrochem. Sci.*, 7 (2012) 10456 – 10475.
9. K.H. Khayat and M. Saric-Coric, *ACI SP-195, Nice*, (2000) 249-268
10. K.H. Khayat and A. Yahia, *ACI Mater. J.*, 94 (1997) 365-372.
11. L. Xu, G. Xu, T. Liu, Y. Chen and H. Gong, *Carbohydr. Polym.*, 92 (2013) 516-522.
12. R. Mbugua, R. Salim and J. Ndambuki, *Case Stud. Constr.*, 5 (2016) 100-111.
13. M. Messali, H. Lgaz, R. Dassanayake, R. Salghi, S. Jodeh, N. Abidi and O. Hamed, *J. Mol. Struct.*, 1145 (2017) 43-54.
14. K. Azzaoui, E. Mejdoubi, S. Jodeh, A. Lamhamdi, E. Rodriguez-Castellon, M. Algarra, A. Zarrouk, A. Errich, R. Salghi and H. Lgaz, *Corros. Sci.*, 129 (2017) 70-81.
15. A. Biswas, P. Mourya, D. Mondal, S. Pal and G. Udayabhanu, *J. Mol. Liq.*, 251 (2018) 470-479.
16. M. Mobin, M. Rizvi, L.O. Olasunkanmi and E.E. Ebenso, *ACS Omega*, 2 (2017) 3997-4008.
17. H. Bentrah, Y. Rahali and A. Chala, *Corros. Sci.*, 82 (2014) 426-431.
18. M. Alwaan and F. Kadhim Mahdi, *Int. J. Chem. Eng.*, (2016)
<http://dx.doi.org/10.1155/2016/5706432>.
19. A. Peter and I. B. Obot, S.K. Sharma, *Int. J. Ind. Chem.*, 6 (2015) 153-164.
20. S. P. Palanisamy, G. Maheswaran, C. Kamal and G. Venkatesh, *Res. Chem. Intermed.*, 42 (2016) 7823.
21. M.G. Sethuraman, V. Aishwarya, C. Kamal and T.J.I. Edison, *Arab. J. Chem.* 10 (2017) 522-530
22. C. Kamal and M.G. Sethuraman, *Ind. Eng. Chem. Res.*, 51 (2012) 10399-10407.
23. C. Kamal and M.G. Sethuraman, *Res. Chem. Intermed.*, 39 (2013) 3813-3828.
24. C. Kamal and M.G. Sethuraman, *Arab. J. Chem.*, 5 (2012) 155-161.
25. Gaussian 09, Revision C. 02, M. J. Frisch, G. W. Trucks, H. B. Schlegel, G. E. Scuseria, M. A. Robb, J. R. Cheeseman, G. Scalmani, V. Barone, B. Mennucci, G.A. Petersson, H.Nakatsuji, M. Caricato, X. Li, H. P. Hratchian, A. F. Izmaylov, J. Bloino, G. Zheng, J. L.Sonnenberg, M. Hada, M. Ehara, K. Toyota, R. Fukuda, J. Hasegawa, M. Ishida, T.Nakajima, Y. Honda, O. Kitao, H. Nakai, T. Vreven, J. A. Montgomery, Jr., J. E. Peralta, F. Ogliaro, M. Bearpark, J. J. Heyd, E. Brothers, K. N. Kudin, V. N. Staroverov, R.Kobayashi, J. Normand, K. Raghavachari, A. Rendell, J. C. Burant, S. S. Iyengar, J.Tomasi, M. Cossi, N. Rega, J. M. Millam, M. Klene, J. E. Knox, J. B. Cross, V. Bakken, C. Adamo, J. Jaramillo, R. Gomperts, R. E. Stratmann, O. Yazyev, A. J. Austin, R.Cammi, C. Pomelli, J. W. Ochterski, R. L. Martin, K. Morokuma, V. G. Zakrzewski, G.A. Voth,

- P. Salvador, J. J. Dannenberg, S. Dapprich, A. D. Daniels, Ö. Farkas, J.B. Foresman, J. V. Ortiz, J. Cioslowski, and D. J. Fox, Gaussian, Inc., Wallingford CT, 2009.
26. Gauss View, Version 5, Ray Dennington, Todd Keith and John Milam, Semichem Inc., Shawnee Mission KS, 2009.
 27. C. Lee, W. Yang and R.G. Parr, *Phys.Rev. B*, 37 (1988) 785–789.
 28. R.G. Pearson, *Inorg. Chem.*, 27 (1988) 734–740.
 29. R.G. Pearson, *Proc. Natl. Acad. Sci.*, 83 (1986) 8440-8441.
 30. R.G. Parr, L.V. Szentpaly and S. Liu, *J. Am. Chem. Soc.*, 121 (1999) 1922-1924.
 31. G. Venkatesh, M. Govindaraju, C. Kamal, P. Vennila and S. Kaya, *RSC Adv.*, 7 (2017) 1401-1412.
 32. P. Vennila, M. Govindaraju, G. Venkatesh, C. Kamal, Y. Sheena Mary, C. Yohannan Panicker, S. Kaya, Stevan Armarkovi and Sanja J. Armarkovi, *J. Mol. Struct.*, 1151 (2018) 245-255.
 33. G. Venkatesh, C. Kamal, P. Vennila, M. Govindaraju, Y. Sheena Mary, Stevan Armarkovi, Sanja J. Armarkovi, S. Kaya and C. Yohannan Panicker, *J. Mol. Struct.*, 1171 (2018) 253-267.
 34. M.A. Quraishi, I. Ahamada, A. Kumar Singha, S. Kumar Shuklaa, B. Lal and V. Singh, *Mater.Chem.Phy.*, 112 (2008) 1035–1039.
 35. M.M. Mennucci, E. P. Banczek, P. R. P. Rodrigues and I. Costa, *Cem. Concr. Compos.*, 31 (2009) 418-424.
 36. M.G. Hosseini, M. Ehteshamzadeh and T. Shahrabi, *Electrochem. Acta*, 52 (2007) 3680–3685.
 37. F. Bentiss, M. Traisnel and M. Lagrenee, *Corros. Sci.*, 42 (2000) 127–146.
 38. A.K. Satapathy, G. Gunasekaran, S.C. Sahoo, K. Amit and P.V. Rodrigues, *Corros. Sci.*, 51 (2009) 2848.
 39. Gengfang Xie and Liu Wei, Inhibitor Effect of *Anthocleista djalensis* Extract on the Corrosion of Concrete Steel Reinforcement, *Int. J. Electrochem. Sci.*, 13 (2018) 5311 – 5322.
 40. S. P. Palanisamy, G. Maheswaran, A. Geetha Selvarani, C. Kamal and G. Venkatesh, *Ricinus communis* – A green extract for the improvement of anti-corrosion and mechanical properties of reinforcing steel in concrete in chloride media, *J. Build. Eng.*, 19 (2018) 376-383.
 41. G. Venkatesh, M. Govindaraju, P. Vennila and C. Kamal, *Theor. Comp. Chem.*, 15 (2016) 1650007.
 42. P. Vennila, M. Govindaraju, G. Venkatesh and C. Kamal, *J. Mol. Struct.*, 1111 (2016) 151-156.
 43. Jianmei Jiao, Xia Xin, Jinglin Shen, Z. Song, Zengchun Xie and Guiying Xu, *RSC Adv.*, 6 (2016) 94373-94381.
 44. M. Lebrini, M. Lagrenee, H. Vezin, L. Gengembre and F. Bentiss *Corros. Sci.*, 47 (2005) 485-505.
 45. S. Deng, X. Li, *Corros. Sci.*, 64 (2012) 253-262.
 46. H. Ma, S. Chen, B. Yin, S. Zhao and X. Liu, *Corros. Sci.*, 45 (2003) 867-882.
 47. M. El Azhar, M. Traisnel, B. Mernari, L. Gengembre, F. Bentiss and M. Lagrenee, *Appl. Surf. Sci.*, 185 (2002) 197–205.
 48. P. Vennila, S. Kavitha, G. Venkatesh and P. Madhu, *Der Pharma Chem.*, 7 (2015) 275-283.
 49. C.A. Loto, *Corros.*, 48 (1992) 759-763.
 50. C.A. Loto and E.T. Odumbo, *Corros.*, 45 (1989) 553-557.
 51. J. Olusegun Okeniyi, C. Akintoye Loto and A.P. Idowu Popoola, *Int. J. Electrochem. Sci.*, 10 (2015) 9893 – 9906.